Quintet State Electron Spin Resonance Spectra of Pyridyldinitrenes

Sergei V. Chapyshev,*,† Richard Walton,‡,§ Paul R. Serwinski,‡,⊥ and Paul M. Lahti*,‡

Institute for Chemical Physics, Chernogolovka, Russia, and Department of Chemistry, University of Massachusetts, Amherst, Massachusetts 01003

Received: March 19, 2004; In Final Form: May 5, 2004

A number of 2,4- and 2,6-diazidopyridine derivatives were photolyzed under frozen matrix conditions (77 K), and their X-band electron spin resonance spectra (ESR) investigated. Typically, both mononitrene and dinitrene spectral features were observed. Cyano substituents reduced or eliminated spectral intensities, especially of the dinitrenes. The 2,4-dinitrenes were readily distinguished from 2,6-dinitrenes, since the major ESR resonance of the former typically occurred at about 3000 G, while that of the latter typically occurred at about 3300 G. Spectral line shape simulations suggest that the 2,6-dinitrenes have consistently larger zero-field splitting (zfs) than the related 2,4-dinitrenes. The 2,4-dinitrenes are estimated to have zfs of $|D/hc| \sim 0.21-0.24$ cm^{-1} and $|E/hc| \sim 0.03-0.04$ cm^{-1}, and the 2,6-dinitrenes to have zfs of $|D/hc|_Q \sim 0.24-0.27$ cm^{-1} and $|E/hc|_Q \sim 0.040-0.05$ cm^{-1}. The difference in spectral behavior is attributed to perturbation of spin density distributions and geometry-influenced interactions between the nitrene units in the 2,4- vs the 2,6-connectivities. Other substitutions on the pyridine had only small effects on the ESR spectra, although the photoefficiency of nitrene and dinitrene production was affected.

Introduction

Numerous workers have been interested in the effects of π-heteroatom substitution upon the electronic natures of conjugated high spin molecules.[1] Nitrogen-containing heterocyclic high-spin compounds have attracted considerable attention. For example, Dougherty and co-workers[2] showed that while pyridinediyl-linked bis-trimethylenemethane system **1** (Chart 1) has a high-spin ground state in accord with simple parity-based expectations, the protonated pyridiniumdiyl system **1**-**NH**$^+$ shows more complicated behavior attributed to a lower multiplicity ground state. Koga, Iwamura, and co-workers showed that complexes **2** with paramagnetic metals give hybrid d−p conjugated systems that exhibit strong exchange between spin sites through the pyridyl rings.[3] Interestingly, efforts to obtain related quintet pyridyl 2,4- and 2,6-dicarbenes **3** and **4** gave singlet spin ground states, apparently due to heteroatom perturbation effects in the pyridine.[4]

In comparison to triplet carbenes, triplet nitrenes have much larger energy gaps between ground high-spin and excited low-spin states (18−22 kcal/mol against 0−5 kcal/mol for carbenes).[5] For this reason, we anticipated that 2,4- and 2,6-pyridyldinitrenes would exhibit high-spin quintet ground spin-states and display ESR spectra similar to those of related quintet *m*-phenylenedinitrenes.[6] The quintet dinitrenes **5** and **6** with *s*-triazine cores are structurally related to the pyridyldinitrenes and have been reported, but appear to be photochemically quite reactive.[7] In previous work we have reported the generation of 2,4- and 2,6-dinitrene byproduct spectra during investigation of 2,4,6-trinitrenopyridines **7** and **8**, as well as generation of the 2,4-dinitrene derived from triazide **9**.[8] In this work, we report the ESR spectra of several quintet pyridyl 2,4- and 2,6-dinitrenes obtained by the photolysis of diazidopyridines **10a**,**b**, **11a**−**e**, **12a**−**c**, **13a**,**b** in frozen solutions. As we show below, results from this large set of examples shows a substantial effect of the substitution pattern on the dinitrene ESR spectroscopy, allowing definitive identification of 2,4- vs 2,6-pyridyldinitrenes. The 2,6-pyridyldinitrenes exhibit ESR spectra significantly different from all of those we know to have been reported in the previous literature for *m*-phenylenedinitrenes, demonstrating that different regioplacement of the nitrene units in an asymmetric π-system like pyridine can have a substantial effect on interelectronic exchange in these quintet states.

Results

Starting Materials. Diazides **10a**,**b**,[9] **11a**−**e**,[10] **12a**−**c**,[11] and **13a**,**b**[12] and triazide **9**[13] were all prepared by literature procedures.

Sample Photolyses. In a typical procedure, 1−5 mg of a diazide sample was dissolved in freshly distilled 2-methyltetrahydrofuran (MTHF), placed in a 5 mm o.d. quartz ESR tube, subjected to 3-fold freeze−pump−thaw degassing, and the tube sealed under vacuum. The sample tube was cooled to 77 K to form a glass, photolyzed for 1−5 min through a Pyrex filter with a 1000 W xenon arc lamp while frozen at 77 K, transferred quickly into a liquid nitrogen cooled quartz finger dewar, and placed in the cavity of a Bruker ESP-300E spectrometer. ESR spectra were then obtained at about $\nu = 9.6$ GHz using 0.2 to 200 mW power levels.[14] Figure 1 shows spectra derived from photolysis of the 2,4-diazide precursors, as well as a comparison to the similar spectrum derived from **9**. Figure 2 shows spectra derived from photolysis of the 2,6-diazide precursors. Mononitrene and dinitrene spectral features are identified in the figures, as well as $g \sim 2$ features attributed to radical byproducts that are frequently formed under these photolytic conditions. In some cases, dinitrene features were only identifiable as new

† Institute for Chemical Physics.
‡ University of Massachusetts.
§ Present address: Ethox Chemicals LLC, Greenville, SC 29605.
⊥ Present address: Sensor Research and Development Corp, Farmington, CT 06034.

10.1021/jp048764e CCC: $27.50
Published on Web 07/14/2004

CHART 1

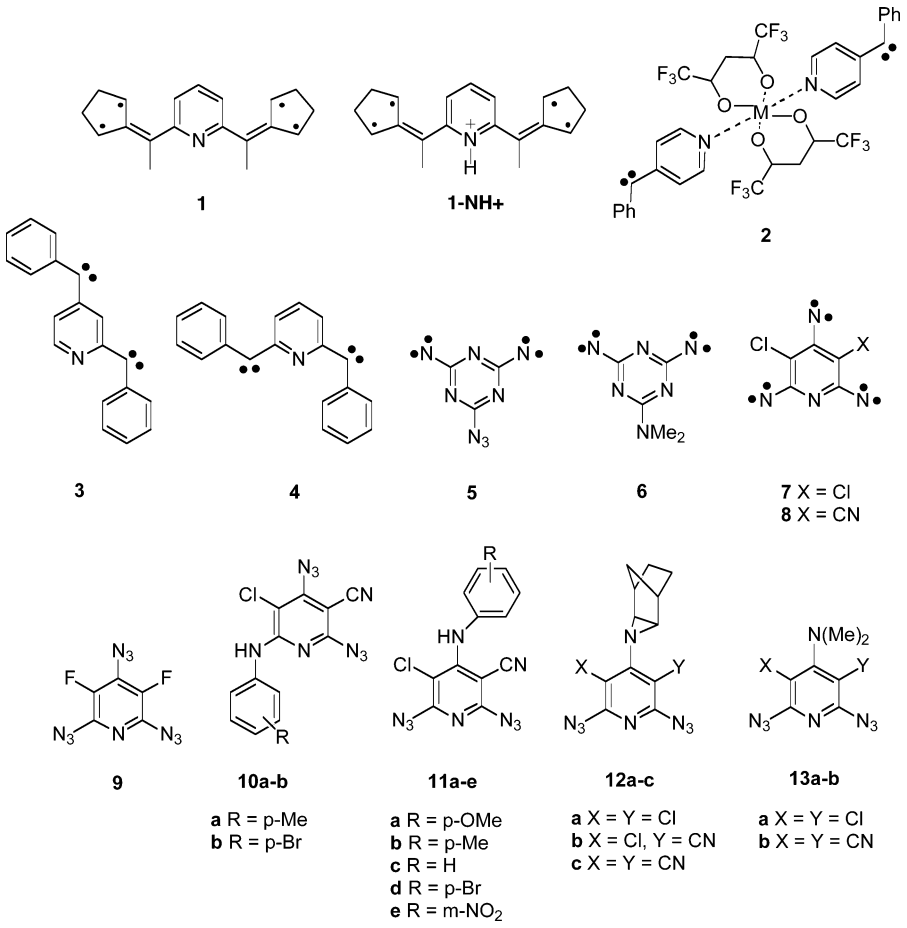

shoulders on the low field portion of the $g \sim 2$ region. The spectral features assigned to the mononitrene and dinitrene intermediates disappeared upon brief thawing and refreezing of the matrices. The thawing procedure typically was accompanied by changes in color of the sample, by gas evolution, and sometimes by formation of a reddish precipitate (probably the result of nitrene polymerization to poly(azopyridine) type products).

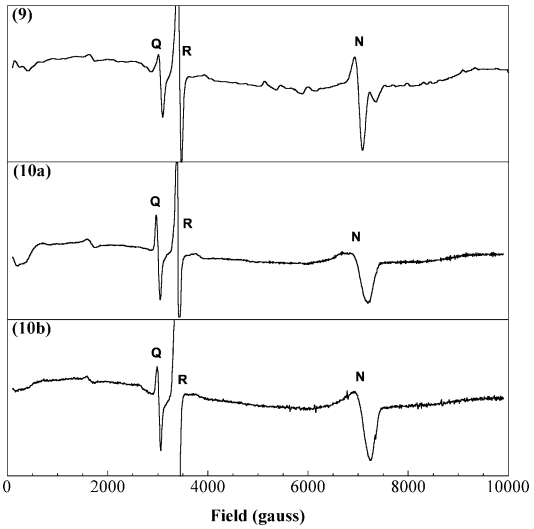

Figure 1. X-band ESR spectra from photolysis of **9** and 2,4-diazido precursors **10a**,**b** (structure numbers are indicated on each spectrum). Spectra were obtained at 77 K in 2-methyltetrahydrofuran. R = radical impurity, N = mononitrene, and Q = quintet dinitrene.

Spectral Analysis. The main types of spectral features identifiable in this study were as follows: triplet state mononitrene *x*,*y*-transitions at about 6800−7100 G; 2,4-pyridyldinitrene quintet state peaks dominated by a major resonance at about 3000 G; 2,6-pyridyldinitrene quintet state peaks dominated by a major resonance at about 3300 G, just to low field or partially overlapping the radical impurity peak in the $g \sim 2$ region. We simulated spectral line shapes by the eigenfield method[15] to estimate zero field splitting (zfs) parameter ranges for the mononitrene and some dinitrene features. This is a useful means of analyzing X-band ESR spectroscopy for large values of $|D/hc|$ in many cases.[15c] Table 1 summarizes the experimental observations and gives the mononitrene zfs parameters.

Discussion

Zero-Field Splitting in Dinitrenes. To illuminate the discussions of dinitrene zfs given below, a brief summary is appropriate. Wasserman noted[16] in the first ESR study of a frozen matrix dinitrene quintet state that the zfs of these systems can be considered as arising from dipolar interaction between component mononitrene sites. The quintet zfs **D**-tensor, $\mathbf{D}_Q$, can be formulated by eq 1, based upon one-center zfs terms $\mathbf{D}_T^a$ and $\mathbf{D}_T^b$ from the component triplet mononitrenes (in our case), and a cross-term for interactions between the spin sites, $\mathbf{D}_T^{ab}$. The one-center interactions are quite strong in nitrenes, so $\mathbf{D}_T^a$, $\mathbf{D}_T^b \gg \mathbf{D}_T^{ab}$, and to a good approximation the quintet **D**-tensor can be modeled solely in terms of the one-center terms, eq 2. The tensor sum of the one-center terms is related to the angle of interaction between the mononitrene **D**-tensors, which is structurally related to the angle θ between the C−N bonds that

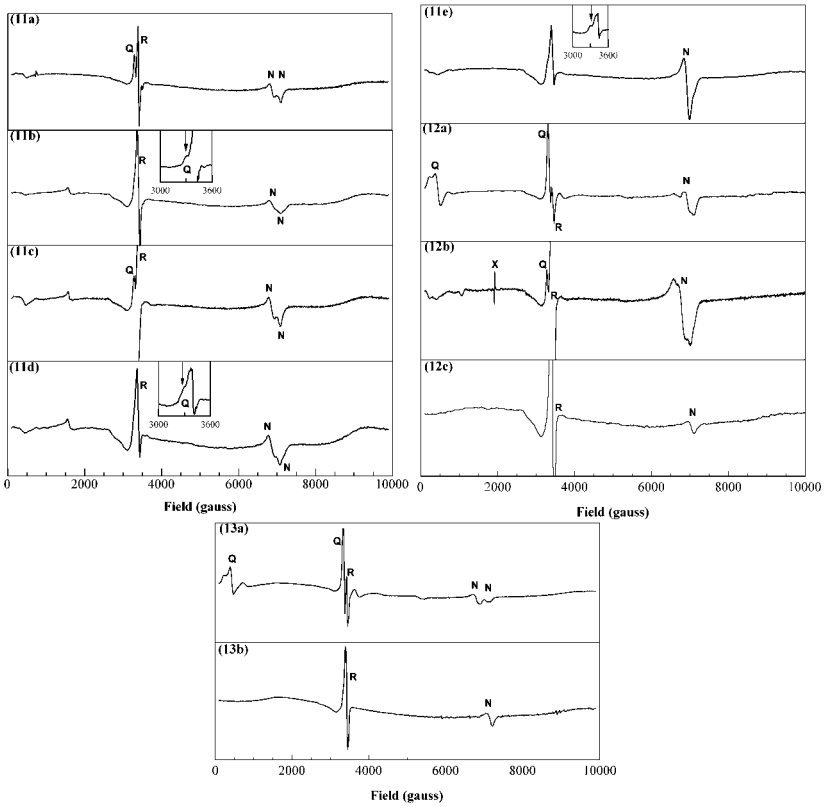

Figure 2. X-band ESR spectra from photolysis of 2,6-diazido precursors **11a**−**e**, **12a**−**c**, **13a**,**b** (structure numbers are indicated on each spectrum). Spectra were obtained at 77 K in 2-methyltetrahydrofuran. R = radical impurity, N = mononitrene, Q = quintet dinitrene, and X = background artifact.

TABLE 1: ESR Peaks Formed from Polyazide Photolyses

precursor	mononitrene zfs	major quintet dinitrene peak position (G)	predicted dinitrene Zfs[a]
9	$\|D/hc\| = 1.01$ cm^{-1}	3050	$D/hc = 0.221$ cm^{-1}
	1.11		$E/hc = -0.045$ cm^{-1}
10a	∼1.01 (broad)	3003	$D/hc = 0.211$ cm^{-1}
			$E/hc = -0.043$ cm^{-1}
10b	∼1.05 (broad)	3030	$D/hc = 0.219$ cm^{-1}
			$E/hc = -0.044$ cm^{-1}
11a	0.99	∼3330	$D/hc = 0.212$ cm^{-1}
	1.04		$E/hc = -0.043$ cm^{-1}
11b	0.97	3315[b]	$D/hc = 0.209$ cm^{-1}
	1.03		$E/hc = -0.042$ cm^{-1}
11c	0.97	∼3330	$D/hc = 0.210$ cm^{-1}
	1.04		$E/hc = -0.042$ cm^{-1}
11d	0.97	3330[b]	$D/hc = 0.209$ cm^{-1}
	1.03		$E/hc = -0.042$ cm^{-1}
11e	1.00[c]	3310[b]	$D/hc = 0.209$ cm^{-1}
			$E/hc = -0.043$ cm^{-1}
12a	1.01	3340	$D/hc = 0.221$ cm^{-1}
	1.05		$E/hc = -0.042$ cm^{-1}
12b	0.95	3280[b]	$D/hc = 0.206$ cm^{-1}
	1.02		$E/hc = -0.041$ cm^{-1}
12c	1.03	*d*	
13a	0.94	3365	$D/hc = 0.207$ cm^{-1}
	1.04		$E/hc = -0.042$ cm^{-1}
13b	1.07	*d*	

[a] On the basis of theoretical eq 2 and experimental mononitrene zfs from first column, assuming that $\theta = 120°$ and $|E/hc| \leq 0.002$ cm^{-1}. [b] Designates position of major quintet peak maximum, where the derivative peak zero point is obscured. [c] Possible second peak shoulder at high field range is not well-resolved. [d] No peak observed.

interact to give the quintet dinitrene state. Aryldinitrenes are now known to follow this relationship quite well,[17] to the point that the quintet zfs parameters D_Q and E_Q can be extracted by line shape simulations and predicted using the zfs terms $D_T(a)$, $E_T(a)$ and $D_T(b)$, $E_T(b)$ for the mononitrene units, assuming structurally reasonable interaction angles θ. For the remainder

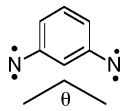

of this article, the paradigm of eq 2 will be assumed, and the details of estimating D_Q and E_Q from mononitrene D_T and E_T will follow literature models.[15,17]

$$\mathbf{D}_Q = \frac{1}{6}(\mathbf{D}_T^a + \mathbf{D}_T^b) + \frac{1}{3}\mathbf{D}_T^{ab} \quad (1)$$

$$\mathbf{D}_Q \cong \frac{1}{6}(\mathbf{D}_T^a + \mathbf{D}_T^b) \quad (2)$$

Quintet Spectra from 2,4-Pyridyldiazides. In principle, the photolysis of the 2,4-diazides **10a**,**b** can yield triplet mononitrenes **14a**,**b** and **15a**,**b** and quintet dinitrenes **16a**,**b** (Scheme 1). The scheme shows formation of the quintets by sequential

SCHEME 1: Photolysis of the 2,4-Pyrdiyldiazides

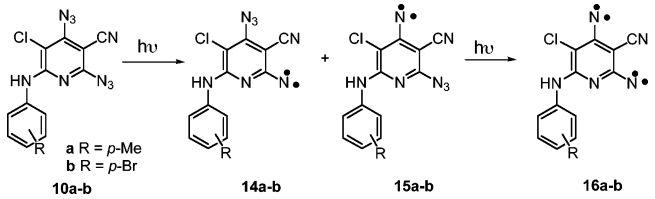

one-photon processes, although one photon, double deazetation is in principle possible. Only one, broad triplet mononitrene

ESR peak is seen at about 6980−7100 G for photolysis at $\lambda >$ 300 nm, suggesting preferential photolysis of one azido group. The peak positions corresponds to $|D/hc|_T \sim 1.0-1.1$ cm^{-1}. Previous studies[18] (including photolysis of 2-azidopyridine model systems) support the formation of the 2-pyridylnitrenes **14a**,**b** under these conditions, which has been explained in terms of fast adiabatic photodissociation of the more labile α-azido groups.[18d,e] The pyridyl-nitrenes have zfs with $|D/hc| \sim 1.0$ cm^{-1} and small E values, with roughly 10% variation due to substituents on the ring system and with 2-pyridylnitrenes apparently having a slightly smaller zfs than 4-pyridylnitrenes. Electron-acceptor substituents tend to increase the zfs, but not much above $|D/hc| \sim 1.1$ cm^{-1}.

Photolysis of **10a**,**b** also forms peaks assignable to quintet dinitrenes **16a**,**b**, especially a major peak at about 3000 G (Figure 1). Similar ESR spectra have been reported from photolysis of *m*-linked aromatic diazides, and assigned to quintet dinitrenes by comparison to spectra such as those derived from **17** and **18**.[6,16a,19] The zfs parameters of **17**[17a] and **18**[20] were

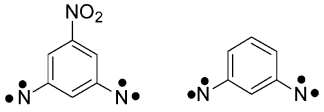

17 **18**

determined by eigenfield spectral simulations[15] to be $|D/hc| = 0.224$ cm^{-1}, $|E/hc| = 0.038$ cm^{-1}, and $|D/hc| = 0.206$ cm^{-1}, $|E/hc| = 0.041$ cm^{-1}, respectively. These examples typify the sort of variation expected for two nitrenes interacting with an angle of about 120°, as given by eq 2 in the preceding section. Assuming that the model of eq 2 holds, the similarity of the ESR spectra of **16a**,**b** to those of **17** and **18** makes sense. The triplet zfs of the mononitrene peaks from **10a**,**b** correspond to $|D/hc|_T \sim 1.0-1.1$ cm^{-1}. Applying eq 2 with $\theta = 118-122°$ yields estimated zfs parameters of $|D/hc|_Q = 0.200-0.238$ cm^{-1} and $|E/hc|_Q = 0.040-0.044$ cm^{-1}, quite similar to the zfs estimated for **17** and **18**. Thus, the 2,4-pyridyldinitrenes seem quite similar to *m*-phenylenedinitrenes in terms of ESR spectroscopic behavior.

Quintet Spectra from 2,6-Pyridyldiazides. The frozen solution photolysis of diazides **11a**−**e**, **12a**,**b**, and **13a** led to the appearance of ESR signals assignable to triplet mononitrenes and peaks at about 3300 G (Figure 2). In some cases, the latter peak is only visible as a shoulder on the low field side of the radical impurity peak at 3350−3400 G ($g \sim 2$) that is typically produced during the frozen solution photolysis. The mononitrene regions for these samples all show two overlapping peaks corresponding to $|D/hc|_T \sim 0.94-1.07$ cm^{-1}, as evaluated by spectral simulation. The lower field mononitrene peaks from **11a**−**e** were assigned to nitrenes **19a**−**e**, those at higher fields

SCHEME 2: Photolysis of the 2,6-Pyrdiyldiazides

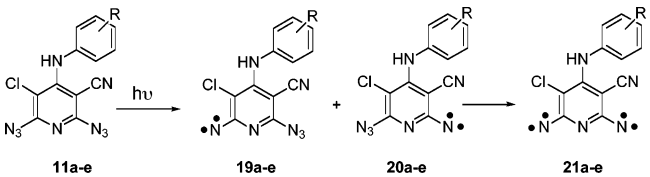

11a-e **19a-e** **20a-e** **21a-e**

a R = *p*-OMe; **b** R = *p*-Me; **c** R = H; **d** R = *p*-Br; **e** R = *m*-NO_2

to nitrenes **20a**−**e**. Both nitrenes are thus formed by cleavage of the labile azido groups in the 2,6-positions, and are spectrally similar save for perturbation by nearby chloro and cyano substituents, hence the signal overlap.

No 2,4-dinitrene can be formed from **11a**−**e**, and no peaks are observed at about 3000 G analogous to those described earlier. However, new peaks are formed at about 3300 G, and they are assigned to quintet dinitrenes **21a**−**e**. Some of these are not clearly resolved but can be assigned as definite shoulders on the low field ranges of the asymmetric, broadened overall peaks caused by overlap of the quintet and the radical resonances; these shoulders are definitely absent in spectra that cannot form 2,6-dinitrenes. Only quintet $S = 2$ peaks derived from **11a**−**e** seem plausible in this region, especially since the 3300 G features are only observed in photolysis of 2,6-pyridyldiazides. Although the relative C−N/C−N angles θ for the 2,6-dinitrenes **21a**−**e** should be very similar to those for the 2,4-dinitrenes **16a**−**e**, the position of the main quintet spectral peak is quite different in these two connectivities.

The difference is interesting, since eq 2 relates the quintet zfs to the mononitrene zfs and the angle θ, both of which are similar for the 2,4- and 2,6-pyridyldinitrenes. It is difficult to evaluate the differences, since there are no simple structural analogues for the 2,6-pyridyldinitrenes. One of the closest is the dinitrene **5** generated by photolysis of **22**,[21] which was

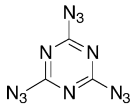

22

estimated in a single-crystal environment to have zfs parameters of $|D/hc|_Q = 0.280$ cm^{-1} and $|E/hc|_Q = 0.058$ cm^{-1}; the mononitrene derived from this system has $|D/hc|_T = 1.40$[21] -1.44[22] cm^{-1}. The X-band ESR spectrum attributed to dinitrene **5** shows its major peak at about 3300 G, a substantially higher field than observed for 1,3-phenylenedinitrenes. Both the mononitrene and dinitrene from **22** have large D values, apparently because the *s*-triazine ring forces π-spin density onto the nitreno nitrogens, increasing the one-center exchange contribution to the zfs. The quintet zfs parameters are consistent with a *meta*-geometry dinitrene having the observed mononitrene zfs interacting according to eq 2.

On the basis of the position of the major quintet state resonance at ∼3300 G, the 2,6-dinitrene zfs expected from eq 2 for **21a**−**e** is $|D/hc|_Q = 0.24-0.27$ cm^{-1} and $|E/hc|_Q = 0.04-0.05$ cm^{-1}. These zfs are a bit smaller than our previous best estimates[8] for 2,6-pyridyl-dinitrenes derived from triazides **23** and **24**, but larger than observed for *meta*-aryldinitrenes such

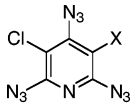

23 X = Cl
24 X = CN

as **17** and **18**. Comparing to the quintet zfs estimates in the previous section of $|D/hc|_Q = 0.200-0.238$ cm^{-1} and $|E/hc|_Q = 0.042-0.044$ cm^{-1} arising from mononitrene $|D/hc|_T \sim 1.0-1.1$ cm^{-1} ($|E/hc|_T \sim 0$ cm^{-1}) with $\theta = 118-122°$, the observed spectra fit the higher range of expectations from eq 2 fairly well. Figure 3 shows a simulation with $S = 2$, $|D/hc|_Q = 0.240$ cm^{-1} and $|E/hc|_Q = 0.047$ cm^{-1} compared to the spectrum generated from **13a**. The comparison is quite good. Even larger values of D/hc and E/hc can be fit to the 3300 G peaks for the 2,6-dinitrenes, but would imply significant deviation from the model of eq 2. Although the qualitative differences between

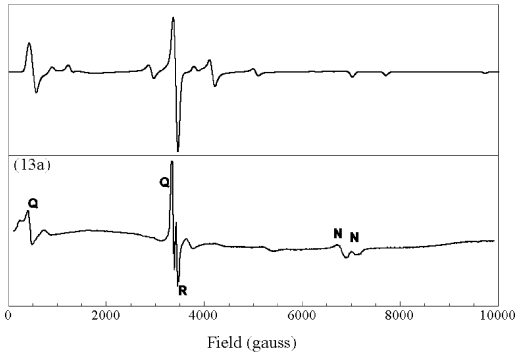

Figure 3. Eigenfield simulation of line shape for a spectrum with $S = 2$, $D/hc = 0.247$ cm^{-1}, and $E/hc = 0.52$ cm^{-1} (upper curve). By comparison, the spectrum derived from 77 K photolysis of **13a** is shown (lower curve). R = radical impurity, N = mononitrene, and Q = quintet dinitrene.

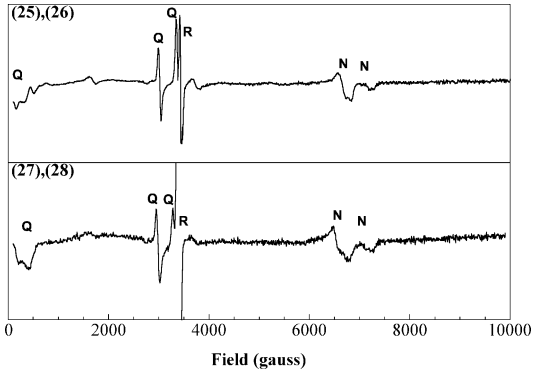

Figure 4. X-band ESR spectra from photolysis of mixtures of **25**/**26** (upper curve) and **27**/**28** (lower curve). Spectra were obtained at 77 K in 2-methyltetrahydrofuran. R = radical impurity, N = mononitrene, Q = quintet dinitrene.

the 2,4- and 2,6-pyridinediyl dinitrenes are experimentally easy to distinguish, there is inherent quantitative imprecision in estimating their zfs using X-band spectra. The spectral fitting is quite sensitive to both D and E values, and distortion of line shapes in the experimental spectra can make it difficult to assign peaks that are weak or broadened. Given the success of the dipolar model of eq 2, we feel that zfs parameters in the ranges $|D/hc|_Q = 0.24-0.27$ cm^{-1} and $|E/hc|_Q = 0.04-0.05$ cm^{-1} are in reasonable accord with the observed spectroscopy of the 2,6-pyridyldinitrenes.

Whatever imprecision there may be in estimating precisely the zfs of the 2,6- by comparison to the 2,4-pyridyldinitrenes, the substantial *qualitative* differences in their ESR spectra allow easy differentiation of the two types of intermediate. The difference between the positions of the main peaks at 3000 G for the 2,4-dinitrenes and at 3300 G for the 2,6-dinitrenes is too large to be due to previously precedented variation in *meta*-arylenedinitrene ESR spectroscopy. We are aware of no other examples of *meta*-arylenedinitrenes that give the major peak at other than 3000 ± 100 G, save for structurally related dinitrene **5** derived from **22** mentioned above.

The clear differentiation of the 2,4-dinitrene from the 2,6-dinitrene spectra is exemplified by the spectra generated (Figure 4) by frozen solution photolysis of **25**/**26** and **27**/**28**, pairs of

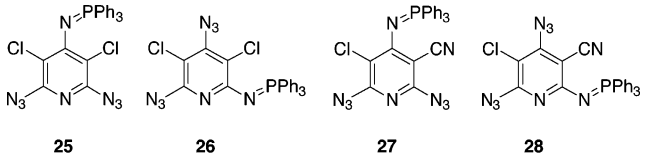

mixed-regiochemistry adducts that are formed by reaction of triphenylphosphine with the corresponding triazides **23** and **24**. Both 3000 and 3300 G peaks are clearly seen in these spectra, clearly indicating formation of both 2,4- and 2,6-dinitrenes.

Ring Substitution Effects on Pyridyldiazide Photolysis. The placement of chloro and cyano substituents affects the photolability of both the precursor azides and the product nitrenes and dinitrenes. Multiple cyano substitution in particular affects the photochemistry. Unlike **12a**,**b** and **13a**, dicyano diazides **12c** and **13b** (Scheme 3) gave weak ESR signals only of triplet

SCHEME 3: Photolysis of Cyano-Substituted 2,6-Pyrdiyldiazides

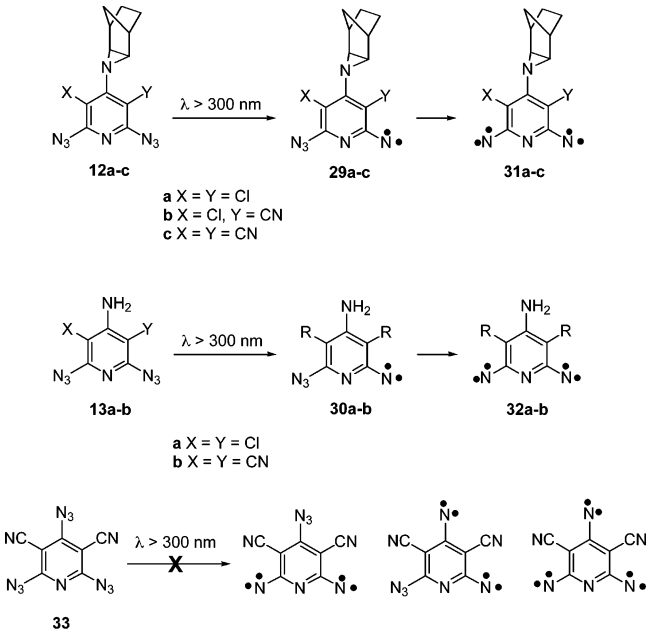

mononitrenes **29b** and **30b**. The absence of spectral evidence for dinitrenes **31c** and **32b** suggests that these dinitrenes are photochemically labile and readily rearrange into ESR-silent species in the course of the photolysis. Similarly, in a previous study[8] we found that diazide **33** gave no ESR peaks consistent with dinitrene or trinitrene formation, but only a weak mononitrene peak.

Triazide **9** gave peaks assignable to nitrenes **34** and **35**, plus a quintet 2,4-pyridyldinitrene **36**.[8] There is no evidence sup-

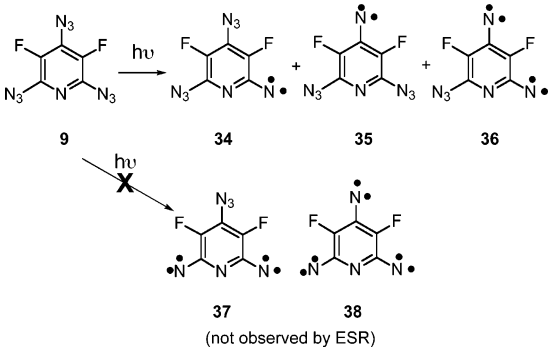

porting formation of 2,6-dinitrene **37**, although such a peak might by coincidence be completely hidden under the $g \sim 2$ radical impurity. Unlike **23** and **24**, **9** does not show ESR peaks consistent with a trinitrene (**38**). Possibly the 2,6-dinitrene and trinitrene derived from **9** are especially photolabile, decomposing to ESR-silent products in a manner similar to the cyano-substituted analogues, as is further described below.

Other studies show photorearrangement of arylnitrenes, in addition to the well-known formation[23] of rearrangement products from initial photolysis of aryl azides themselves. For example, dicyanophenylnitrene **39**, readily rearranges into **40**

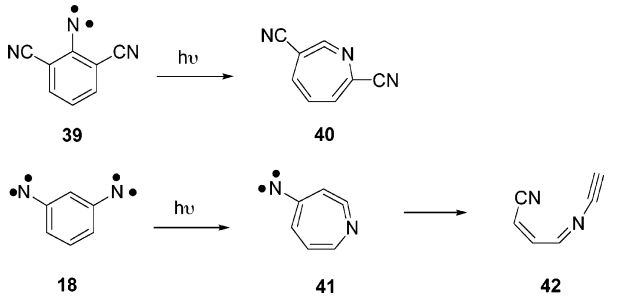

during photolysis.[24] Even the unsubstituted dinitrene **18** apparently can rearrange into **41** and **42** upon extended photolysis, as suggested by FTIR studies in Ar matrices.[25] The lack of dinitrene and trinitrene ESR peaks from **23**, **24**, and **33** is not due to sluggish photolysis, since FTIR studies have shown that the azide group absorptions in cyano-substituted pyridyl azides decrease upon photolysis, apparently leading to ring-expansion products and not nitrenes.[18c] Therefore, we presume that rearrangement is a main pathway that limits or precludes the observation of dinitrenes in cases the cyano-substituted systems.

Spectral Differences in 2,4- vs 2,6-Pyridyldinitrenes. All of our data show that there is a consistent, characteristic difference in the ESR spectra derived from the 2,4- vs the 2,6-pyridyldiazides. Explaining the difference is somewhat more challenging. As mentioned earlier, one expects the zfs in dinitrenes to be largely controlled by the one-center exchange interactions on the mononitrene units. The one-center interactions are in turn most affected by variations in the π-spin density on the nitrene. One does not expect large variation in the localized σ-spin density on the nitrene, but any variations here will also have an effect on zfs, given the strong interaction with the π-spin density. Thus, any systematic effect on the nitrene spin density distribution could have a commensurate effect on zfs. Finally, as described earlier, one also expects the vector angle between the interacting mononitrene units to influence the zfs, due to the dipolar nature of the quintet zfs tensor.

Although quantitating the zfs dinitrenes **16** and **21** is not straightforward for reasons discussed earlier, we considered possible systematic trends that differ between the 2,4- and 2,6-regioconnectivities. UB3LYP/6-31G* quintet state computations[26−28] summarized in Figure 5 show Mulliken spin populations and bond lengths for parent 2,4- and 2,6-pyridyldinitrene quintet states, as well as 1,3-phenylenedinitrene, **18**. The nitrene site spin densities in the 2,4-dinitrene are smaller than those in the 2,6-dinitrene, and closer to those of **18**. This would help explain why the 2,4-dinitrene quintet ESR spectrum more closely resembles those of **18** and related *m*-arylenedinitrenes. If this trend accurately represents the experimental spin densities and the mononitrene spin densities were the sole variable contributing to zfs, the 2,6-dinitrenes would then have large zfs than the 2,4-dinitrenes.

Of course, the real situation is more complex, with a variety of spin densities contributing to the total zfs. In addition, the geometric effect of the vector angle *between* the interacting nitrenes also needs to be considered. The computational trends of our previous work and in this study show that the vector angles of the 2,6-dinitrenes are somewhat smaller than those of the 2,4-dinitrenes. For example, in the model systems of Figure 5, the 2,6-dinitrene C−N/C−N vector angle is 117.3°,

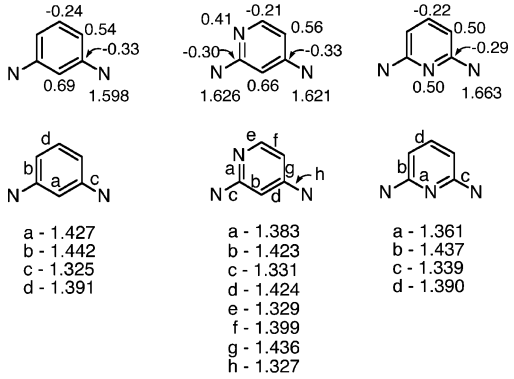

Figure 5. Mulliken spin density distributions (upper) and selected bond lengths (lower, Å) for UB3LYP/6-31G* optimized quintet states of model 2,4- and 2,6-pyridyldinitrenes. Computations were carried out using Gaussian03[26] and Spartan 2002.[27]

and the 2,4-dinitrene angle is 122.8°. Applying eq 2 above, and assuming (for ease of comparison) the same mononitrene zfs for both interacting spin sites, the smaller vector angle would yield a smaller predicted quintet zfs *D* value and a larger *E* value.

These observations are suggestive rather than definitive. Substituent effects in each individual case should influence the spin density distributions in mononitrene units of the different pyridyldinitrenes, and will probably also affect the dinitrene C−N/C−N vector angles. It is not clear how spin density and geometric factors will interact in contributing to the experimental zfs. Quantitative prediction of the zfs of either the mononitrenes or dinitrenes is thus beyond the scope—and capability—of this study. However, the computational *trends* in nitrene spin density populations and C−N/C−N vector angles as functions of the placement of nitrene units on a pyridine ring suggest that these factors consistently differ between the 2,4- and 2,6-pyridyldinitrenes, leading to consistent differences in their observed ESR quintet spectra.

Conclusions

Photolysis of a number of substituted diazidopyridines in frozen solution at 77 K gave X-band ESR spectra of mononitrenes and dinitrenes. 2,4-Pyridyldinitrenes show ESR resonances that are very similar to those previously observed for *m*-arylenedinitrenes, but 2,6-pyridyldinitrenes give significantly different spectra, consistent with larger zero field splitting in the latter. Both general categories of spectra can be explained in terms of previously described models of dipolar interaction between the nitrene spin units, assuming that differing amounts of spin delocalization from the nitrenes into the pyridine ring at different ring positions influence the zero field splitting in the 2,6-dinitrenes. The distinctive difference in ESR spectra of the 2,4- vs 2,6-pyridyldinitrenes makes their identification straightforward in cases where both can be formed. In addition, the differences demonstrate that variation of heteroatom placement in π-isoconjugate structural units can substantially perturb interactions between open-shell units in a spectroscopically observable manner, despite the expected similarity of molecular geometry. The results imply that the use of heterocycles should allow a fairly wide tunability in the exchange behavior and spin-state related chemistry of high spin, open-shell molecules and related systems.

Acknowledgment. Financial support of this work by the National Science Foundation (NSF CHE-9521594, CHE-

9740401, and CHE-0109094) is gratefully acknowledged. We thank Prof. K. Sato for use of the eigenfield ESR line shape fitting programs[15c] EFT and MKSPC.

Supporting Information Available: Tables of summary optimized geometry and Mulliken spin population data for UB3LYP-6-31G* computations of the quintet states of 2,4-pyridyldinitrene, 2,6-pyridyldinitrene, and 1,3-phenylenedinitrene. This material is available free of charge via the Internet at http://pubs.acs.org.

References and Notes

(1) For example, see discussions in: (a) Borden, W. T.; Iwamura, H.; Berson, J. A. *Acc. Chem. Res.* **1994**, *27*, 109. (b) Lahti, P. M. In *Molecule-Based Magnetic Materials. Theory, Techniques, and Applications*; Turnbull, M. M., Sugimoto, T., Thompson, L. K., Eds.; ACS Symposium Series 644; American Chemical Society: Washington, DC, 1996; p 218.

(2) West, A. P., Jr.; Silverman, S. K.; Dougherty, D. A. *J. Am. Chem. Soc.* **1996**, *118*, 1452.

(3) (a) Karasawa, S.; Kumada, H.; Koga, N.; Iwamura, H. *J. Am. Chem. Soc.* **2001**, *123*, 9685. (b) Takano, Y.; Kitagawa, Y.; Onishi, T.; Yoshioka, Y.; Yamaguchi, K.; Koga, N.; Iwamura, H. *J. Am. Chem. Soc.* **2002**, *124*, 450 and references therein.

(4) Bae, J. Y.; Yano, M.; Sato, K.; Shiomi, D.; Takui, T.; Kinoshita, T.; Abe, K.; Itoh, K.; Hong, D. *Mol. Cryst. Liq. Cryst.* **1999**, *334*, 59.

(5) (a) Borden, W. T.; Gritsan, N. P.; Hadad, C. M.; Karney, W. L.; Kemnitz, C. R.; Platz, M. S. *Acc. Chem. Res.* **2000**, *33*, 765. (b) Chapyshev, S. V. *Mendeleev Commun.* **2002**, 168.

(6) A summary of recent dinitrene studies is given in: Nimura, S.; Yabe, A. In *Molecular Magnetism in Organic-Based Materials*; Lahti, P. M., Ed.; Marcel Dekker: New York, 1999; p 127ff.

(7) (a) Chapyshev, S. V. *Mendeleev Commun.* **2003**, 53. (b) Sato, T.; Narazaki, A.; Kawaguchi, Y.; Niino, H.; Bucher, G. *Angew. Chem., Int. Ed.* **2003**, *42*, 5206.

(8) Chapyshev, S. V.; Walton, R.; Sanborn, J. A.; Lahti, P. M. *J. Am. Chem. Soc.* **2000**, *122*, 1580.

(9) Chapyshev, S. V.; Ibata, T. *Heterocycles* **1993**, *36*, 2185.

(10) Chapyshev, S. V.; Chapysheva, N. V. *Chem. Heterocycl. Compd.* **1994**, *30*, 585.

(11) (a) Chapyshev, S. V. *Chem. Heterocycl. Compd.* **1993**, *29*, 1426. (b) Chapyshev, S. V.; Anisimov, V. M. *Chem. Heterocycl. Compd.* **1997**, *33*, 1315. (c) Chapyshev, S. V. *Mendeleev Commun.* **1999**, 164.

(12) Chapyshev, S. V.; Platz, M. S. *Mendeleev Commun.* **2001**, 56.

(13) Chapyshev, S. V. *Chem. Heterocycl. Compd.* **1999**, *35*, 632.

(14) For more details about the ESR spectroscopy of azidopyridines, see: Walton, R. Ph.D. Dissertation, University of Massachusetts, Amherst, MA 1998.

(15) (a) Teki, Y. Ph.D. Dissertation, Osaka City University, Osaka, Japan 1985. (b) Teki, Y.; Takui, T.; Yagi, H.; Itoh, K.; Iwamura, H. *J. Chem. Phys.* **1985**, *83*, 539. (c) Sato, K.; Ph.D. Dissertation, Osaka City University, Osaka, Japan 1992. (d) See a summary and examples of eigenfield ESR line shape analysis in: Takui, T.; Sato, K.; Shiomi, D.; Itoh, K. In *Molecular Magnetism in Organic-Based Materials*; Lahti, P. M., Ed.; Marcel Dekker: New York, 1999; p 197ff. (e) Belford, G. G.; Belford, R. L.; Burkhalter, J. F. *J. Magn. Reson.* **1973**, *11*, 251.

(16) Wasserman, E.; Murray, R. W.; Yager, W. A.; Trozzolo, A. M.; Smolinsky, G. *J. Am. Chem. Soc.* **1967**, *89*, 5076.

(17) (a) Fukuzawa, T. A.; Sato, K.; Ichimura, A. S.; Kinoshita, T.; Takui, T.; Itoh, K.; Lahti, P. M. *Mol. Cryst. Liq. Cryst., Sect. A* **1996**, *278*, 253. (b) Kalgutkar, R. S.; Lahti, P. M. *J. Am. Chem. Soc.* **1997**, *119*, 4771. (c) Kalgutkar, R. S.; Lahti, P. M. *Tetrahedron Lett.* **2003**, *44*, 2625.

(18) (a) Evans, R. A.; Wong, M. W.; Wentrup, C. *J. Am. Chem. Soc.* **1996**, *118*, 4009 and citations in ref 7 therein. (b) Wentrup, C.; Kuzaj, M.; Lüerssen, H. *Angew. Chem., Int. Ed. Engl.* **1986**, *25*, 480. (c) Chapyshev, S. V.; Kuhn, A.; Wong, M. H.; Wentrup, C. *J. Am. Chem. Soc.* **2000**, *122*, 1572. (d) Chapyshev, S. V.; Walton, R.; Lahti, P. M. *Mendeleev Commun.* **2000**, 7. (e) Chapyshev, S. V.; Walton, R.; Lahti, P. M. *Mendeleev Commun.* **2000**, 187.

(19) However, the appearance of *meta*-linked dinitrenes depends on theirconformations, if a strictly *meta*-geometry is not enforced by the structure. See: Murata, S.; Iwamura, H. *J. Am. Chem. Soc.* **1991**, *113*, 5547. Lahti, P. M.; Minato, M.; Ling, C. *Mol. Cryst. Liq. Cryst.* **1995**, *271*, 147 and discussions in ref 6.

(20) (a) Oda, N.; Sato, K.; Shiomi, D.; Kozaki, M.; Okada, K.; Takui, T. *Proceedings of International Symposium on Reactive Intermediates and Unusual Molecules* (ISRIUM-2001); Nara, Japan 2001; p 117. (b) Chapyshev, S. V.; Enyo, T.; Tomioka, H. *Proceedings of International Symposium on Reactive Intermediates and Unusual Molecules* (ISRIUM-2001); Nara, Japan 2001; p 74.

(21) Nakai, T.; Sato, K.; Shiomi, D.; Takui, T.; Itoh, K.; Koazki, M.; Okada, K. *Mol. Cryst. Liq. Cryst., Section A* **1999**, *334*, 157.

(22) Moriarty, R. M.; Rahman, M.; King, G. J. *J. Am. Chem. Soc.* **1966**, *88*, 842.

(23) See, for example, the summary in: Wentrup, C. *Neutral Reactive Intermediates in Organic Chemistry*, John Wiley: New York, 1984.

(24) Gritsan, N. P.; Likhotvorik, I.; Tsao, M.; Celebi, N.; Platz, M. S.; Karney, W. L.; Kemnitz, C. R.; Borden, W. T. *J. Am. Chem. Soc.* **2001**, *123*, 1425.

(25) Chapyshev, S. V.; Tomioka, H. *Bull. Chem. Soc. Jpn.* **2003**, *76*, 2075.

(26) Frisch, M. J.; Trucks, G. W.; Schlegel, H. B.; Scuseria, G. E.; Robb, M. A.; Cheeseman, J. R.; Montgomery, J. A. J.; Vreven, T.; Kudin, K. N.; Burant, J. C.; Millam, J. M.; Iyengar, S. S.; Tomasi, J.; Barone, V.; Mennucci, B.; Cossi, M.; Scalmani, G.; Rega, N.; Petersson, G. A.; Nakatsuji, H.; Hada, M.; Ehara, M.; Toyota, K.; Fukuda, R.; Hasegawa, J.; Ishida, M.; Nakajima, T.; Honda, Y.; Kitao, O.; Nakai, H.; Klene, M.; Li, X.; Knox, J. E.; Hratchian, H. P.; Cross, J. B.; Adamo, C.; Jaramillo, J.; Gomperts, R.; Stratmann, R. E.; Yazyev, O.; Austin, A. J.; Cammi, R.; Pomelli, C.; Ochterski, J. W.; Ayala, P. Y.; Morokuma, K.; Voth, G. A.; Salvador, P.; Dannenberg, J. J.; Zakrzewski, V. G.; Dapprich, S.; Daniels, A. D.; Strain, M. C.; Farkas, O.; Malick, D. K.; Rabuck, A. D.; Raghavachari, K.; Foresman, J. B.; Ortiz, J. V.; Cui, Q.; Baboul, A. G.; Clifford, S.; Cioslowski, J.; Stefanov, B. B.; Liu, G.; Liashenko, A.; Piskorz, P.; Komaromi, I.; Martin, R. L.; Fox, D. J.; Keith, T.; Al-Laham, M. A.; Peng, C. Y.; Nanayakkara, A.; Challacombe, M.; Gill, P. M. W.; Johnson, B.; Chen, W.; Wong, M. W.; Gonzalez, C.; Pople, J. A. *Gaussian03*, B03 ed.; Gaussian, Inc.: Pittsburgh, PA, 2003.

(27) Spartan 2002 from Wavefunction, Inc., Irvine, CA (http://www.wavefun.com).

(28) (a) Becke, A. D. *J. Chem. Phys.* **1993**, *98*, 5648. (b) Lee, C.; Yang, W.; Parr, R. G. *Phys. Rev. B* **1988**, *37*, 785.